

RESEARCH ARTICLE | JANUARY 12 2023

Polarimetric Thomson scattering measurements in Joint European Torus high temperature plasmas

R. Scannell   ; J. G. Clark  ; Y. Kim  ; D. Kos  ; M. Maslov; L. Giudicotti  ; JET Contributors

 Check for updates

Rev. Sci. Instrum. 94, 013506 (2023)

<https://doi.org/10.1063/5.0128057>


View
Online


Export
Citation

CrossMark



Optimize
Your Research



Use the Optimal Technology for All Vacuum Requirements

PFEIFFER  VACUUM

Polarimetric Thomson scattering measurements in Joint European Torus high temperature plasmas

Cite as: *Rev. Sci. Instrum.* **94**, 013506 (2023); doi: [10.1063/5.0128057](https://doi.org/10.1063/5.0128057)

Submitted: 26 September 2022 • Accepted: 9 December 2022 •

Published Online: 12 January 2023



View Online



Export Citation



CrossMark

R. Scannell,^{1,a)} J. G. Clark,² Y. Kim,¹ D. Kos,¹ M. Maslov,¹ L. Giudicotti,³ and JET Contributors^{b)}

AFFILIATIONS

¹UKAEA/CCFE, Culham Science Centre, Abingdon, Oxon OX14 3DB, United Kingdom

²Department of Electrical Engineering and Electronics, University of Liverpool, Liverpool L69 3GL, United Kingdom

³Department of Physics and Astronomy, Padova University, Via Marzolo 8, 35131 Padova, Italy

^{a)}Author to whom correspondence should be addressed: rory.scannell@ukaea.uk

^{b)}See the author list of “Overview of the JET preparation for deuterium-tritium operation” by E. Joffrin *et al.*, *Nucl. Fusion* **59**, 112021 (2019).

ABSTRACT

Thomson scattered light is polarized in the same orientation as the incident laser beam at low electron temperatures (T_e). At high T_e , part of the spectrum begins to become randomly polarized due to relativistic reasons. First measurements of the depolarized Thomson scattering spectrum were obtained from Joint European Torus (JET) pulses in 2016. This paper builds upon these initial measurements with the data obtained during 2021. These new measurements improve upon first results, in particular, by obtaining spectral measurements of the depolarized spectrum. The recent JET campaign was well suited to these measurements with long and hot plasmas. The resulting data are averaged over many plasmas and laser pulses to obtain a measurement of the amount of “p” and “s” scattered light as a function of T_e . This experimentally obtained $d(p/s)/dT_e$ is then fitted and found to show reasonable agreement with the theoretically predicted depolarized fraction. Error estimates on the measured “p/s” have been obtained and show that the measurements are meaningful. This is good news for ITER for which the intention is to use this measurement as a check on T_e determined by the core plasma Thomson scattering diagnostic by using conventional spectral measurement techniques.

Published under an exclusive license by AIP Publishing. <https://doi.org/10.1063/5.0128057>

I. INTRODUCTION

The ITER Core Plasma Thomson Scattering (CPTS) diagnostic is required to measure up to 40 keV.¹ This implies measuring down to wavelengths of ~ 400 nm using conventional or “spectral” Thomson scattering² from a 1064 nm laser. This short wavelength requirement arises due to the broad spectral width at $T_e = 40$ keV at the large CPTS scattering angles of $\sim 160^\circ$ in the core. Measuring at short wavelengths is challenging as many of the expected losses due to the neutron or radiation damage of optics or fibers will be largest in this region (400–700 nm). Similarly, line emission will be largest in this same wavelength region.

Polarimetric Thomson scattering is an alternative Thomson scattering technique not currently deployed on existing machines. It takes advantage of the fact that a small fraction of the Thomson

scattering spectrum becomes depolarized at high electron temperature (T_e). The depolarization increases with T_e for a given scattering angle and is uniform across the spectrum. These properties mean that an increase in the lower wavelength limit, due to losses or line emission, would not impact the ability to infer T_e from polarimetric measurements. In fact, polarimetric measurements would be immune to any potential unquantified systematics in spectral transmission, provided that the spectral transmission is not polarization dependent.

The technique of polarimetric Thomson scattering was first proposed in Ref. 3. Since then, there have been significant advances in the theoretical basis.^{4–6} The expected amount of depolarization may now be readily determined for given T_e and scattering angle. In a spectral Thomson scattering system, the injected light is typically orthogonal or “s” polarized (perpendicular) with respect to the

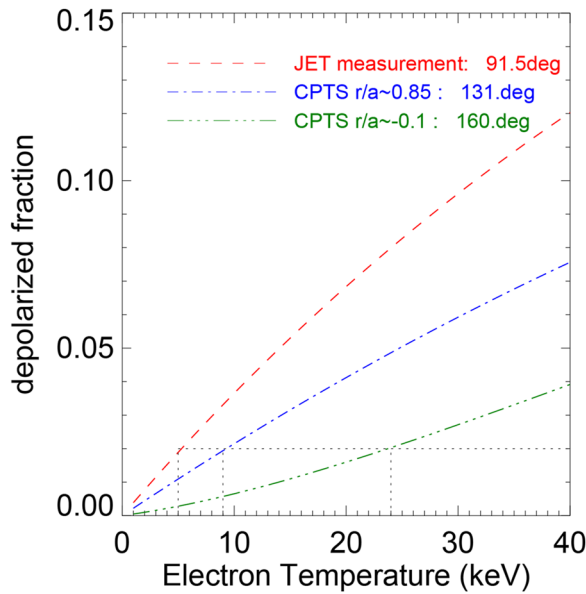


FIG. 1. Fraction of light depolarized as a function of electron temperature for the scattering angle of JET measurements and for the two extreme scattering angles of the ITER CPTS diagnostic.

scattering plane formed by incident and scattering vectors. Depolarized light is randomly polarized and therefore equal in both “s” and “p” (parallel) polarizations. In a spectral Thomson scattering system, “p” polarized light is often removed by polarizers as it is considered to contain background light but no scattered light. For a polarimetric Thomson scattering system, the “s” and “p” components of the scattered light are separately measured and quantified and the ratio of the two (“p/s”) is used to infer T_e .

At a 90° scattering angle, the fraction of light in the non-standard “p” polarization increases approximately linearly at $0.191\%/keV$ as calculated from theoretical predictions in the range 1–10 keV. The JET data that are considered in this paper are taken at a scattering angle of 91.4° and up to temperatures of ~ 9 keV from the conventional HRTS (high resolution Thomson scattering)⁷ diagnostic, as opposed to the JET LIDAR diagnostic. Hence, for these scattering events, a p/s ratio of up to $\sim 1.72\%$ is expected at $T_e = 9$ keV. The ITER CPTS diagnostic operates from $\sim 131^\circ$ at the low field side edge, $r/a \sim 0.85$, to $\sim 160^\circ$ at the plasma center. The depolarization is significantly less at a 160° scattering angle such that the JET results at 6 keV are approximately equivalent to ITER results at 20 keV. This is illustrated in Fig. 1, which shows the relative sensitivity at these two scattering angles. The CPTS system will allow for more averaging than JET as it is based on a 100 Hz rather than a 20 Hz laser and with longer plasma pulse durations. Additionally, the ITER system can provide polarimetric measurements over multiple spatial points compared to at just one point for JET.

II. INSTALLATION ON JET

The first polarimetric Thomson scattering measurement on a fusion machine was obtained on JET during the DD campaign in 2016, from pulses 92 038–92 504.⁸ We will refer to these

measurements as DD in contrast to our recent measurements during DT. This campaign was the second Deuterium–Tritium (DTE2) campaign on JET since the initial DT campaign in 1997 and as such had a goal to maximize the fusion energy produced. This led to long high temperature plasmas, which were particularly suitable for the polarimetric measurements. From the initial results during DD, the ratio of “p” to “s” light was obtained as a function of T_e by taking each pulse and averaging the scattered signals from that JET pulse during the heating phase. These results indicated that polarimetric Thomson scattering works as a technique and is in line with theoretical predictions.

The motivation for new measurements during the DT campaign is as follows:

- Significant variation in the p/s ratio was observed in the DD measurements. This is inherent from the fact that the number of “p” scattered photons is very low and motivates further measurements to confirm the initial result. Estimating the uncertainty on the determined $d(p/s)/dT_e$ in these new measurements was another key goal.
- After the initial measurements during DD, a Raman calibration was performed. The result of this calibration implied a significant difference in the sensitivity of the fiber with the “p” polarizer vs that of the fiber with the standard “s” polarizer. This arose from the fact that the “s” fiber was misaligned to the laser beam, making it ~ 6.7 times less sensitive to scattered light. This has now been corrected, and in the DT campaign, the two fibers should be equally sensitive.
- The $d(p/s)/dT_e$ value was obtained by a linear fit to the p/s ratio vs T_e for a given pulse number. In the DD measurements, a significant offset was observed at the origin. This offset implied that a phenomenon such as stray laser light was causing some measurement in the “p” channel even at very low T_e . There is a concern that the unknown source of this offset could in some way lead to a systematic error in the measurement of the “p” signal. New polychromators have been used for the DT measurements that are significantly more resilient to stray laser light not only because the filters have stronger optical blocking of the laser line but also because a special transmissive filter was installed as the first cascade in the polychromator. This transmissive filter should transmit (and therefore remove) at least 95% of 1064 nm light, so if the offset in the linear fit to the p/s ratio is produced by stray laser light, it should be significantly reduced.
- The measurements during DD were taken from a single channel polychromator with a laser line notch filter in front of it. The rationale for this was that in order to improve the signal-to-noise ratio, the full scattered spectrum could be measured on a single detector, thereby reducing detector noise. For the measurements during DT, we elected to use a more conventional polychromator design with multiple spectral channels, so $d(p/s)/dT_e$ could be independently calculated for each spectral channel. The rationale for this is that while it would add some extra random noise to the measurements in the form of additional detector noise for each avalanche photodiode (APD) utilized, it would reduce potential systematic error by providing independent measurements.

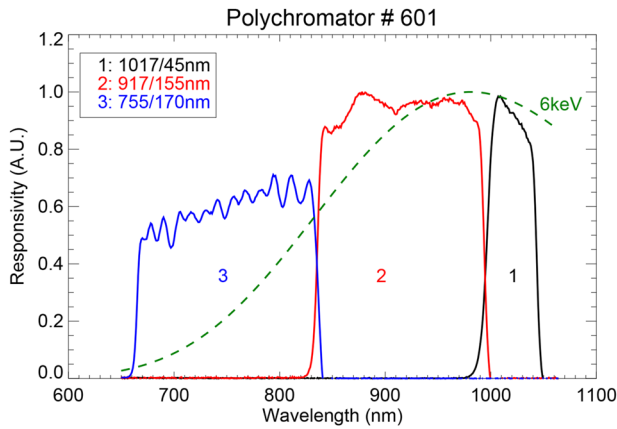


FIG. 2. Spectral responsivity of the polychromator installed to detect “p” polarized light. Also shown is the spectral intensity of the expected light at 6 keV.

The spectral responsivity of the installed polychromator on JET is shown in Fig. 2 with an overlaid modeled 6 keV spectrum at $\theta = \pi/2$. A three-channel polychromator was installed, which should be responsive to temperatures in the $1 \text{ keV} < T_e < 10 \text{ keV}$ range.

The location of the scattering centers for the polarimetric TS spatial point used in this paper and the control point from which spectral T_e is obtained are 2.95 and 2.93 m in major radius, respectively, which is the core of the JET plasma. These points are shown in Fig. 1 of Ref. 8.

III. OVERVIEW OF DATASET

JET pulses during the DT campaign as indicated in Table I form the dataset used to analyze $d(p/s)/dT_e$. These pulses were filtered to remove low temperature pulses as obtaining a good signal-to-noise ratio for the higher JET pulses with high T_e is the limiting factor. The condition for inclusion was at least one second at $T_e > 4 \text{ keV}$ was observed; this corresponds to 20 data points as the HRTS laser operates at 20 Hz. Applying this filtering, 323 JET pulses were selected for the dataset. In all cases, T_e is determined from the HRTS measurement point adjacent to the polarimetric measurements.

Figure 3(a) shows the median T_e observed during the phase of selected shots where T_e is $>4 \text{ keV}$ effectively corresponding to the temperature during the “hot” phase of the pulse. Figure 3(b) shows the duration of time where these pulses were above 4 keV.

Once a JET pulse was selected for the dataset, the full duration of that pulse is used, including the low temperature part of

TABLE I. Key parameters of the JET DT campaign database used for analysis.

Condition for inclusion	$1 \text{ s} > 4 \text{ keV}$
First JET pulse	99 147
Last JET pulse	99 982
No. of JET pulses used	323
No. of HRTS segments $>4 \text{ keV}$	19 051

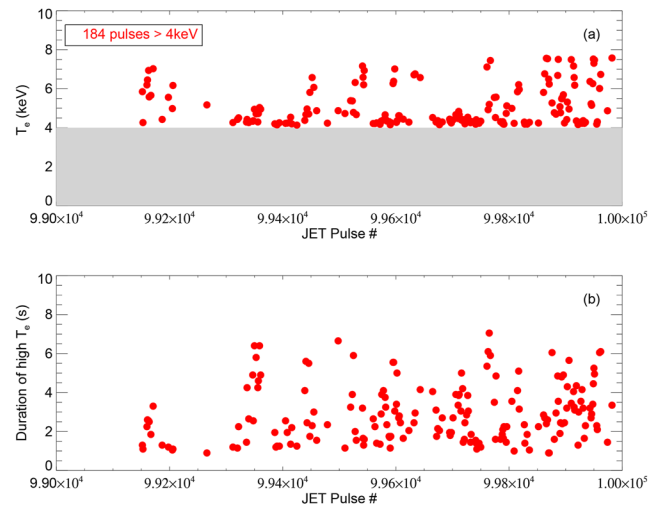


FIG. 3. (a) Median T_e observed during the hot ($>4 \text{ keV}$) phase of JET pulses and (b) duration of the $>4 \text{ keV}$ period of these pulses.

the pulse before the heating phase. Since these low temperature parts of the pulse are significantly longer than the heating phase, there are many low temperature points in the dataset. 16 sequential 0.5 keV temperature “bins” are defined from 1 to 9 keV. Each HRTS measurement time slice is assigned a temperature bin based on the measured HRTS temperature at the most high field side point, which is adjacent to the image of fibers with the dedicated “p,” “s,” and 45° polarizers. The number of HRTS time slices in each bin is shown in Fig. 4. As can be seen, there are $>10\,000$ time slices in the 1–1.5 keV bin and ~ 500 time slices in the 8.5–9 keV bin. The number of time slices in these bins is one of the fundamental limits on our ability to accurately measure the “p/s ratio” and, hence, $d(p/s)/dT_e$.

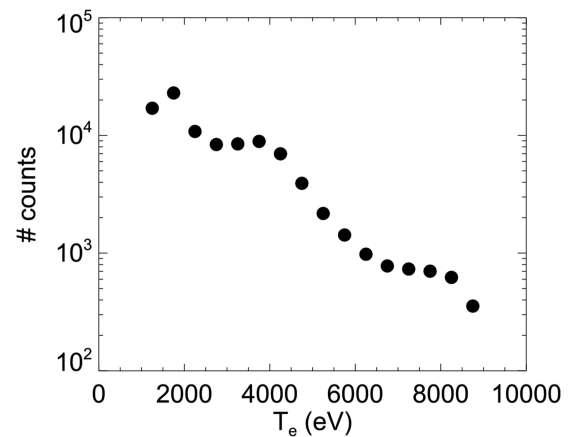


FIG. 4. Number of counts observed in temperature bins of 500 eV width used to construct the dataset.

IV. POLARIMETRIC MEASUREMENTS

Once each time slice is assigned an appropriate T_e bin, as described previously, the signal time traces are then accumulated for that bin and then divided by the number of observations in that bin. The time traces for six of the bins are shown in Fig. 5 to illustrate the data obtained. There are three scattered signal timings corresponding to three delay lines for each time trace as summarized in Table II. The setup used is such that there are six optical fibers combined into a single polychromator. Each pulse corresponds to two fibers, which have identical delay lines and are adjacent in the plasma. The first pulse at ~ 80 ns has scattered light from a single “s” fiber and scattered light from a polarizer oriented at 45° , so $0.5 \times (s + p)$. The second pulse at ~ 220 ns is connected to two fibers measuring “p” polarized light. The third pulse at ~ 380 ns is similar to the first pulse measuring the addition of an “s” and 45° fiber. The time integral of the three pulses is calculated, and the determined ratio of “p/s” used is pulse 2/(pulse 1 + pulse 3), which corresponds to $2 \times p/(3 \times s + p)$, which approximates to $2/3 \times p/s$. Details on the design of the HRTS system and fiber delay lines are given in Refs. 7 and 8.

TABLE II. Fibers used in a polarimetric spectrometer with the corresponding polarizer orientations and scattered signal timings.

Delay line / time (ns)	Fiber 1 polarizer	Fiber 2 polarizer
Delay 1: ~ 80	S	45°
Delay 2: ~ 220	P	P
Delay 3: ~ 380	S	45°

Figure 5 also illustrates the magnitude of the scattered signals obtained in comparison to the noise fluctuations seen outside of the time windows of interest. At low T_e , where averaging is performed over many time slices, the fluctuations are much lower compared to fluctuations observed at high T_e . These time traces indicate an increasing “p” scattered signal with increasing T_e . There is a tendency for low T_e to be correlated with low n_e as the low T_e data are not obtained during the heating phases of JET pulses; hence, a comparison of the “p” and $1\% \times$ “s” pulses also shown in Fig. 5 is required.

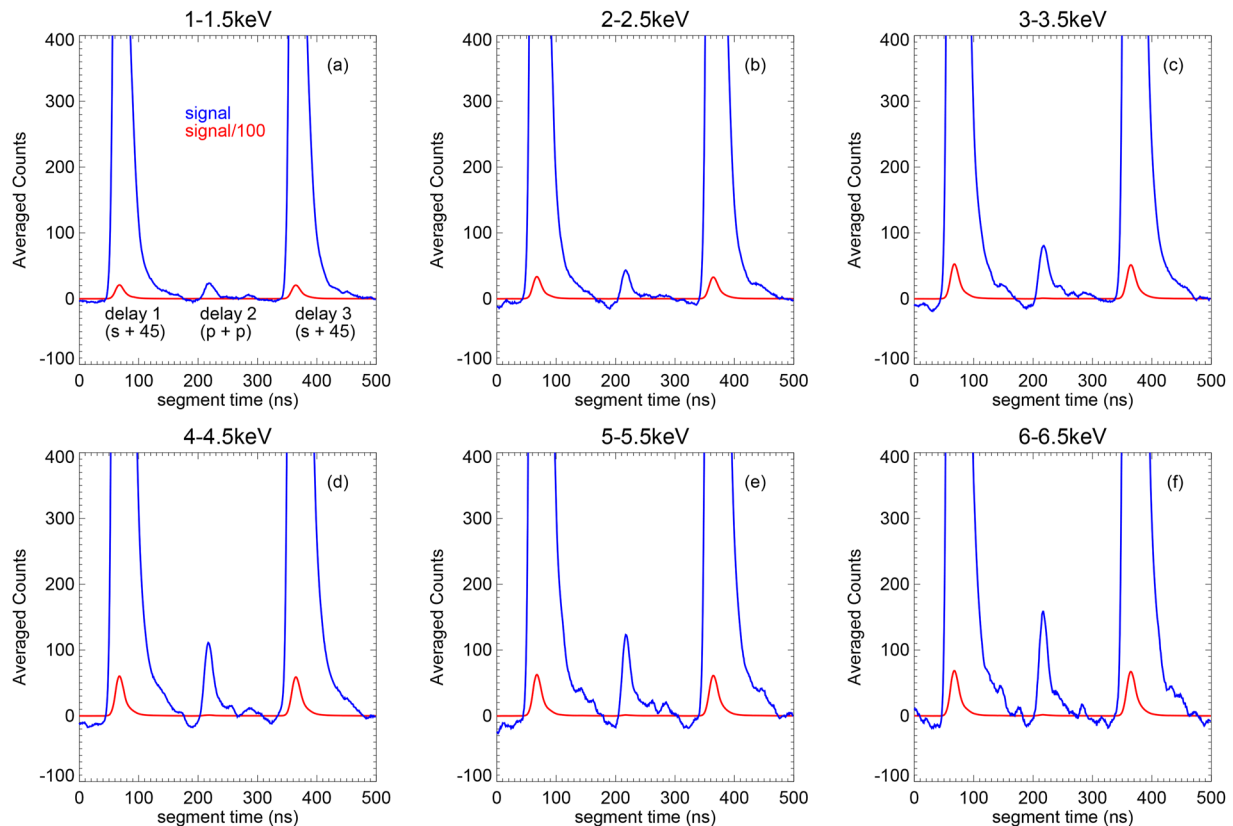


FIG. 5. Time traces of scattered signals observed in spectral channel 2 for six temperature bins accumulated over the full dataset. Each time trace has three pulses with different optical delays. Each pulse comes from two fibers with the same optical delay line. The first and third pulses at ~ 80 and ~ 380 ns, respectively, come from one fiber with an “s” polarizer and one fiber with a 45° polarizer. The second pulse at ~ 210 ns comes from two fibers with “p” polarizers. The fibers are located in adjacent spatial channels in the plasma. In addition to the averaged scattered signal traces a second trace illustrating that 1% of the scattered signal trace is overlaid.

For each JET pulse, HRTS diagnostic data acquisition operates for 259 segments, ~ 13 s, before the plasma when the laser is firing into the vessel. Measurements taken during this time period are used for straylight subtraction. One of the motivations for measurement during the DT campaign was to remove straylight using a high laser line rejection polychromator as it was assumed that the offset observed in DD originated from transmission by the optical filters of light at 1064 nm. The measurements during these 259 segments have subsequently shown that there is a very low measurable straylight

signal in spectral channel 2, but there is a measurable straylight signal in spectral channel 1, which is $\sim 3.4\%$ of the average “s” light observed. For this dataset, the averaged time trace obtained during this 259 segment straylight period has in all cases been subtracted from subsequent measurements obtained with plasmas. This subtraction was performed on a JET pulse to pulse basis. Initially, no subtraction of straylight was performed and the “p/s” ratio obtained from channel 1 was found not to be linear with increasing T_e . This occurred as the measurement was polluted by this straylight, which

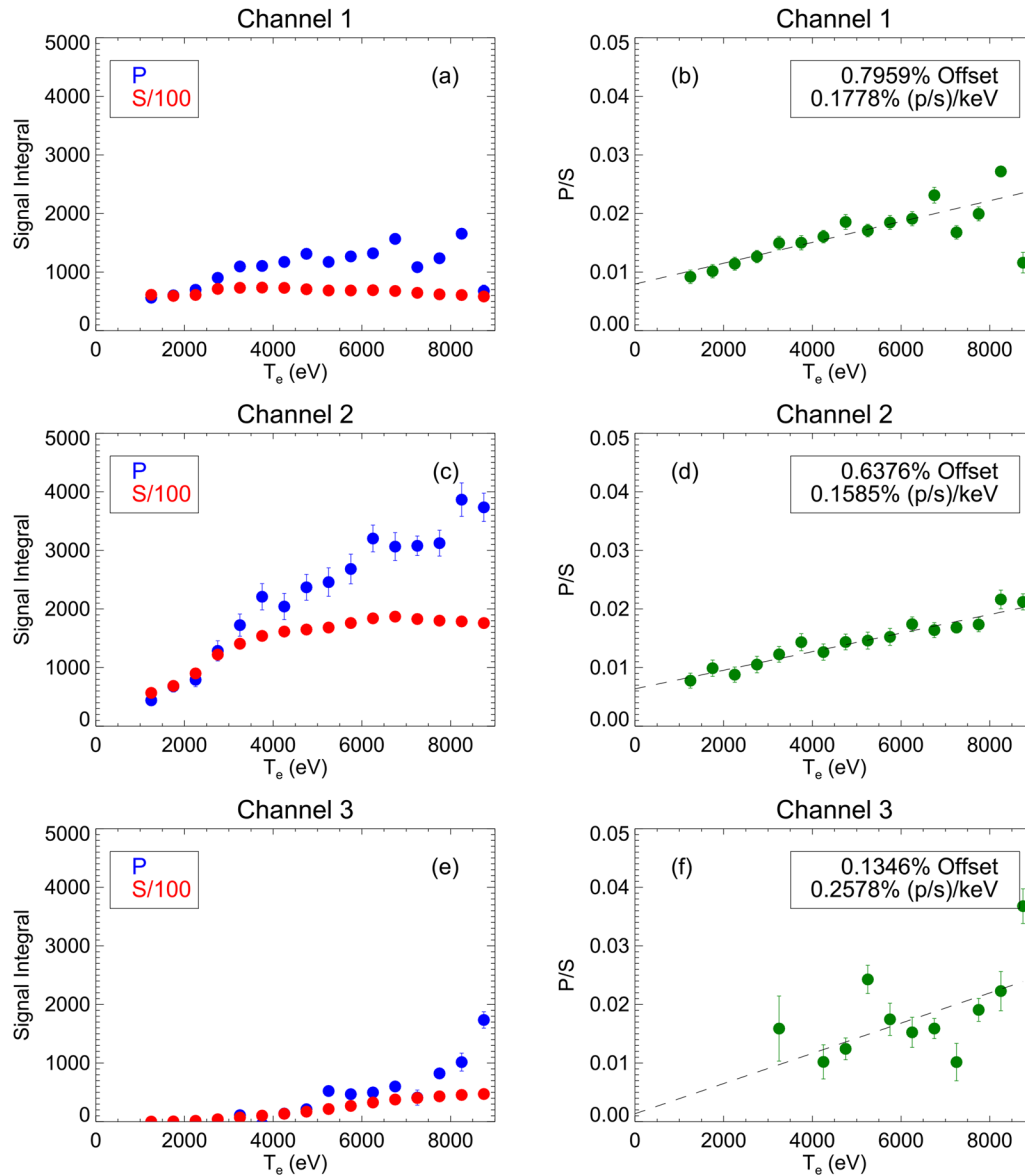


FIG. 6. For spectral channels 1–3, the change in “p” and “s” signal integrals with T_e is shown in (a), (c), and (e), respectively, and the increase in the “p/s” ratio with T_e is shown in (b), (d), and (f). For the plots showing the ratio, a linear fit and best fit parameters of that linear fit are provided in the legend. These data here are determined by accumulating the full 323 pulse dataset in contrast with the values in Fig. 7 obtained from subsets of this full dataset.

TABLE III. Comparison of theoretically and experimentally observed $d(p/s)/dT_e$ for various spectral channels. Uncertainty estimates are obtained from Monte Carlo analysis. Spectral channel 3 is excluded due to large uncertainty.

Light before plasma	Straylight Offset of linear fit	Bleed through	$d(p/s)/dT_e$ (%/keV)
Theoretical prediction	0.185–0.194
Channel 1	3.37%	$0.796\% \pm 0.122\%$	$0.176\% \pm 0.041\%$
Channel 2	0.46%	$0.638\% \pm 0.067\%$	$0.154\% \pm 0.023\%$

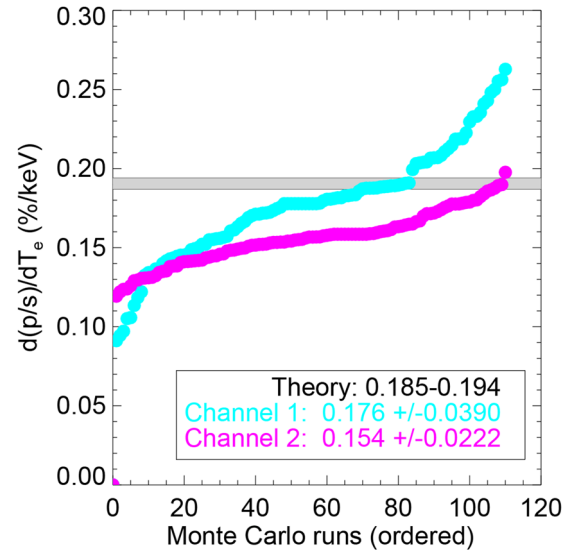
was much larger than the level of “p” signal expected. It was found that the subtraction of the straylight had to be performed on a JET pulse basis in order to obtain a meaningful measurement. This indicates that the straylight level is in fact varying over the plasma pulses observed. It is not clear if the straylight observed in spectral channel 1 is due to the transmission at the laser wavelength or some other in-band source of light related to the laser pulse. In any case, there is much lower straylight observed in spectral channel 2, $\sim 0.46\%$ of the average “s” light, so the data obtained in this channel are not compromised by this.

A comparison of the signal integrals from the “p” and “s” polarizations is shown in Fig. 6(a) for spectral channel 1 (the 1017/45 nm filter). Up to 2 keV, the “p” signal approximately equals 1% of the “s” signal integral. At higher T_e , the “s” signal is relatively flat with T_e , probably a combination of an increasing signal due to higher electron density and a decreasing signal due to T_e shifting the scattered spectrum out of this wavelength band. At these higher T_e , the “p” signal increases faster than the “s” signal. A linear fit to the “p/s” ratio is shown in Fig. 6(b). The slope of the linear fit corresponds well with theoretical predictions of 0.191%/keV. Uncertainties were derived for the p/s values; these uncertainties are based on the scatter in the signal traces where there are no scattered pulses and the expected contribution of this to a signal integral.

A similar comparison is shown in Fig. 6(c) for spectral channel 2. The measurements in this channel show increasing “p” signal levels above and beyond the “s” signals with increasing T_e . The linear fit to the ratio shown in Fig. 6(d) again shows good agreement on the slope with theoretical predictions and some offset at $T_e = 0$. The quality of data for channel 2 appears better than that in channel 1; this might be the case because (a) at the temperatures of interest, there is more signal in spectral channel 2 improving data quality and (b) there is much lower straylight in spectral channel 2 ($\sim 0.46\%$ of the “s” signal) compared with spectral channel 1 ($\sim 3.4\%$ of the “s” signal), which may have an impact on measurements. Results from channel 3 are also shown in Figs. 6(e) and 6(f) for completeness but are not considered as the scattered signal levels are much lower than in channels 1 and 2 and not high enough to provide good “p” signal measurements.

The theoretical estimate of a linear variation of 0.191% $d(p/s)/dT_e$ is a very good approximation. If we numerically determine the derivative, values of $\sim 0.185/\text{keV}\%$ and $\sim 0.194/\text{keV}\%$ are obtained at 1 and 7 keV, respectively. To represent this non-linearity, an error bar has been assigned to the theoretical prediction in Table III.

In order to estimate the uncertainty on the determined $d(p/s)/dT_e$, a Monte Carlo approach was taken. Each Monte Carlo run varied which JET pulses were included such that individual JET

**FIG. 7.** Results of $d(p/s)/dT_e$ from Monte Carlo runs, where individual JET discharges are randomly included or excluded from the dataset in each run. The determined slopes for each run have been arranged in ascending order for each spectral bin for illustrative purposes and comparison with the theoretical values.

pulses were included in each Monte Carlo run with a 50% probability. The full dataset has 323 pulses; hence, each individual Monte Carlo run had ~ 160 pulses. Following the selection for each Monte Carlo run, the data were accumulated in the normal way and the resulting $d(p/s)/dT_e$ parameter and offsets were determined. The results of 100 such Monte Carlo runs are shown in Fig. 7 where the resulting $d(p/s)/dT_e$ is shown for spectral channels 1 and 2. To illustrate the variation in results, the value of $d(p/s)/dT_e$ is plotted in ascending order for each channel. This shows that most $d(p/s)/dT_e$ values determined in spectral channels 1 and 2 are both under the theoretical estimate. For spectral channel 1, the mean value determined is within 1-sigma of the theoretical range. For the spectral channel 2 dataset, the mean value determined is close to 2-sigma away from the theoretical estimate.

V. CONCLUSIONS

The aim of this work was to verify the technique of polarimetric Thomson scattering for use on ITER. Thomson scattering is inherently a difficult measurement to carry out as you need to obtain a rejection of stray laser light of $n_e \times \sigma_{T_e} \sim 10^{-10}$ using the optical

rejection of filters and geometry, which is challenging. Polarimetric Thomson scattering is even more challenging as it is typically a factor of 10^2 below “s” Thomson scattered light, and it is required to distinguish the “p” light from the “s” light. The key measurements obtained in this work are summarized in Table III. The main conclusion of this work is then that $d(p/s)/dT_e$ obtained is close to theoretical predictions as measured independently by two spectral bands of a polychromator. This gives support to the application of this technique on ITER. The discrepancy between the theoretical predictions and experimental measurements is larger than the error bars obtained by including random pulses. We cannot explain this fully, but attribute it to the very small signal levels we are measuring and sensitivities to systematic effects.

The fact that similar results are obtained in spectral channels 1 and 2 despite some $\sim 3.37\%$ straylight being observed in spectral channel 1 indicates that pollution due to straylight observed in previous experiments did not significantly influence those results.

Both spectral channels 1 and 2 see a non-negligible offset signal in the “p” channel that we interpret as “bleed through.” At this low level, a number of origins for this offset are possible. It could be due to the physical accuracy of polarizer installation, laser beam polarization, or extinction ratio of the polarizer. Alternatively, it could be some combination of these phenomena or a different phenomenon such as “scrambling” of the polarisation in the collection optics.

The measurements taken on JET show the variation of p/s with T_e over a few hundred JET pulses and with $\sim 19\,000$ samples over 4 keV. The goal of this technique as applied to ITER is to do the opposite and infer T_e from p/s . JET has one advantage over ITER in the measurement of polarimetric Thomson scattering, it is at a favorable scattering angle. This favorable scattering angle provides $\sim 3\times$ as many photons. ITER has two significant advantages over JET. The core plasma Thomson scattering system will operate at 100 Hz, and it can install measurement samples of polarimetric light across the full laser chord, giving it up to ~ 70 spatial samples compared to a single spatial sample on JET. Hypothetically, then, for a 20 keV peaking profile on ITER, a polarimetric measurement with the equivalent quality to the full $\sim 19\,000$ samples from this JET dataset could be obtained in tens of seconds of an ITER discharge by averaging over a number of spatial points from the core plasma Thomson scattering diagnostic.

ACKNOWLEDGMENTS

The authors would like to thank all the contributors that made the generation of the high temperature pulses on JET used in this publication possible. That includes all those control room staff who were involved in the running of the experiments, such as diagnostic coordinators and session leaders. It also includes all those involved in the design of the pulses, the JET DT task force leaders, and, in

particular, the scientific coordinators: D. Frigione, L. Garzotti, F. Rimini, D. Van Ester, C. Challis, J. Hobirk, A. Kappatou, E. Lerche, D. Keeling, R. Dumont, M. Maslov, P. A. Schneider, Y. Kazakov, M. Nocente, S. Brezinsek, C. Giroud, P. Mantica, S. Sharapov, R. Dumont, M. Fitzgerald, D. King, A. Kirschner, M. Mantsinen, and P. Jacquet.

This work was carried out within the framework of the EUROfusion Consortium, funded by the European Union via the Euratom Research and Training Programme (Grant Agreement No. 101052200—EUROfusion). The views and opinions expressed are, however, those of the authors only and do not necessarily reflect those of the European Union or the European Commission. Neither the European Union nor the European Commission can be held responsible for them. This work was also funded by EPSRC under Grant No. EP/W006839/1.

AUTHOR DECLARATIONS

Conflict of Interest

The authors have no conflicts to disclose.

Author Contributions

R. Scannell: Conceptualization (equal); Data curation (equal); Formal analysis (equal); Investigation (equal); Writing – original draft (equal); Writing – review & editing (equal). **J. G. Clark:** Formal analysis (equal). **Y. Kim:** Conceptualization (equal). **D. Kos:** Investigation (equal). **M. Maslov:** Investigation (equal). **L. Giudicotti:** Formal analysis (supporting).

DATA AVAILABILITY

The data that support the findings of this study are available from the corresponding author upon reasonable request. For further information on the MAST data used, please contact PublicationsManager@ukaea.uk.

REFERENCES

- ¹A. J. H. Donné *et al.*, *Nucl. Fusion* **47**, S337 (2007).
- ²R. Scannell *et al.*, *J. Instrum.* **12**, C11010 (2017).
- ³F. Orsitto and N. Tartoni, *Rev. Sci. Instrum.* **70**, 798 (1999).
- ⁴S. E. Segre *et al.*, *Phys. Plasmas* **7**, 2677 (2000).
- ⁵E. Parke *et al.*, *J. Instrum.* **9**, C02030 (2014).
- ⁶V. V. Mirnov *et al.*, *Phys. Plasmas* **23**, 052108 (2016).
- ⁷R. Pasqualotto *et al.*, *Rev. Sci. Instrum.* **75**, 3891 (2004).
- ⁸L. Giudicotti *et al.*, *Nucl. Fusion* **58**, 044003 (2018).